Epidemic Processes Over Time-Varying Networks

Philip E. Paré, Carolyn L. Beck, and Angelia Nedić

***Abstract*—The spread of viruses in biological networks, computer networks, and human contact networks can have devastating effects; developing and analyzing mathematical models of these systems can provide insights that lead to long-term societal benefits. Prior research has focused mainly on network models with static graph structures; however, the systems being modeled typically have dynamic graph structures. In this paper, we consider virus spread models over networks with dynamic graph structures, and we investigate the behavior of these systems. We perform a stability analysis of epidemic processes over time-varying networks, providing sufficient conditions for convergence to the disease-free equilibrium (the origin, or healthy state), in both the deterministic and stochastic cases. We present simulation results and discuss quarantine control via simulation.**

***Index Terms*—Epidemic processes, Networked systems, Stochastic systems, Time-varying systems.**

I. Introduction

MATHEMATICAL models of epidemics have been studied for hundreds of years. Bernoulli developed one of the first known models inspired by the smallpox virus [1]. Of particular interest to the work discussed herein are the so-called susceptible-infected-susceptible (SIS) models, which have been developed for both continuous- [2]–[6] and discrete-time domains [6]–[8]. These are standard models commonly used to capture the evolution of virus infections in networks. In a basic SIS model, at each time step, each individual node or agent is either *infected* or *susceptible* to infection. A susceptible agent may be infected by neighboring agents with some given infection rate β, where the network graph structure determines the connectivity between agents and, hence, plays a direct role in facilitating or inhibiting the spread of infection. An infected agent may be cured with some given healing rate δ, returning to the susceptible state. The first SIS model, developed by Kermack and McKendrick [2], is given by

$$\begin{aligned}\dot{S}(t) &= -\beta S(t)I(t) + \delta I(t)\\ \dot{I}(t) &= \beta S(t)I(t) - \delta I(t)\end{aligned} \tag{1}$$

where $S(t)$ is the group of susceptible agents and $I(t)$ is the group of infected agents. This model considers the propagation of a virus over a trivial network, that is, it assumes complete connectivity and models the infected and susceptible agents as two aggregated groups.

In [7], Wang *et al.* propose a discrete-time model for virus spread over a nontrivial network and derive an epidemic threshold that guarantees convergence to the disease-free equilibrium (DFE). The authors give a convergence rate in terms of the largest eigenvalue of the adjacency matrix of the network, which is proportional to the ratio of the healing and infection rates. A necessary and sufficient condition for exponential stability of the DFE is provided, with several simulations and results for specific graph structures given. Peng *et al.* [8] provide a necessary and sufficient condition for stability of the DFE for an extension of the model from [7]. Peng *et al.* also discuss possible immunization techniques and formulate a convex optimization problem for forming an optimal immunization strategy, based on a relaxation of the problem constraints. In [6], Ahn and Hassibi study both discrete- and continuous-time SIS models, where both the DFE and the nondisease-free equilibrium (NDFE), sometimes referred to as the endemic equilibrium, are considered, and the existence, uniqueness, and stability conditions for the NDFE are established. In [3], Fall *et al.* analyze a continuous time SIS model, deriving sufficient conditions for global asymptotic stability for both the DFE and the NDFE. Van Mieghem *et al.* [4] expose some limitations of the model presented in [7], namely, that it is only accurate if the infection rate is below the epidemic threshold, that is, the system is tending toward the DFE. The authors propose a 2^n-state Markov chain model and an n-intertwined Markov chain model as alternatives to the model in [7] and explore their stability properties by studying the limiting cases of the complete graph and the line graph. These two models will be explained in more detail in the following section. Preciado *et al.* use geometric programming ideas [9], in [10] and [11], to develop optimal vaccination techniques for the continuous-time model from [4]. Pasqualetti *et al.* [12] apply a network control technique to a discretized linearized version of the model from [4]. In [13] and [14], Khanafer *et al.* further explore the stability properties of the equilibria of the continuous-time model from [4] and propose an antidote control technique. For a survey of this area, see [15]. The aforementioned papers consider only static graph structures. Although contributing to

Manuscript received January 6, 2017; revised March 22, 2017 and April 28, 2017; accepted May 4, 2017. Date of publication May 18, 2017; date of current version September 17, 2018. This work was supported by the National Science Foundation (NSF) under Grants ECCS 15-09302, CCF 0904619, and DMS 13-12907. All material in this paper represents the position of the authors and not necessarily that of the NSF. Recommended by Associate Editor Q. Zhao. *(Corresponding author: Philip E. Paré.)*

P. E. Paré and C. L. Beck are with the Coordinated Science Laboratory, University of Illinois at Urbana–Champaign, Urbana, IL 61801 USA (e-mail: philip.e.pare@gmail.com; beck3@illinois.edu).

A. Nedić is with the School of Electrical, Computer and Energy Engineering, Arizona State University, Tempe, AZ 85281 USA (e-mail: angelia@illinois.edu).

Digital Object Identifier 10.1109/TCNS.2017.2706138

the understanding of virus spread and the ensuing eradication, in most of the cases, static graph structures are fundamentally too simple to capture the essential dynamics of infectious disease processes. Most of the applications that motivate these systems have agents that are mobile, which implies that the underlying graph structure is time varying. For example, computer networks are comprised of smart phones, laptops, and other mobile devices, which connect to different devices as they move around. In order to obtain a better understanding of these systems, a more realistic representation, that of *virus dynamics over time-varying networks*, is necessary.

The previous work on virus spread over time-varying networks is limited to unweighted and undirected graphs. In [16], Prakash *et al.* extend the discrete-time model used in [7] to a model with a time-varying graph structure. The authors provide a sufficient condition for local exponential stability of the origin (the DFE) and propose a control scheme that removes agents from the system. In [17], Bokharaie *et al.* provide similar results to those in [16], extending the model from [7] to the time-varying case and proving local exponential convergence to the origin. The authors state that these results extend to the continuous-time-varying case, without proof. The authors of both [16] and [17] consider unweighted undirected graphs and extend the model from [7], which was shown in [4] to have significant shortcomings. In [18], Rami *et al.* extend the model from [3] to that of a switching virus model. The authors provide a sufficient condition for stability of the DFE, show the existence of a periodic NDFE, and give a sufficient condition for stability of the DFE for a Markovian switching virus model. Sanatkar *et al.* [19] present results similar to the ideas in [18], but for a discrete-time model. Liu [20], also following the ideas in [18], examines a switching susceptible-infected (SI) model for a system with trivial graph structures [i.e., similar to the model in (1)]. In [21], Ogura and Preciado propose a less general version of the results given in [5, Prop. 1], examining a subset of random graphs and giving sufficient conditions for almost sure global exponential stability. Somewhat related results can also be found in the physics/network science literature, including, but not limited to, the papers [22]–[25]. In these papers, less general time-varying models are studied with some analysis provided.

In this paper, we propose notable extensions to the models from [4] to include time-varying, weighted, directed, and undirected graph structures. To the best of our knowledge, we are the first to derive results for weighted and directed time-varying graph structures. We provide sufficient conditions for global exponential stability of the DFE for these models. We compare the 2^n-state Markov chain model and n-intertwined Markov chain model via simulations for both static graphs and time-varying graphs. We present additional simulations that give insight into stability and quarantine control results and, from these, formulate several corollaries.

A preliminary version of these results is given in [5]. Further contributions of this paper include the following:

1) the development of conditions for global exponential convergence to the DFE for heterogeneous viruses over directed time-varying networks;
2) the development of conditions for exponential convergence to the DFE for heterogeneous viruses over directed time-varying networks that do not require the linearized system to always be strictly Hurwitz;
3) extensions of the time-varying virus models to a *stochastic framework* with accompanying stability results;
4) an in-depth evaluation of the effectiveness of the n-intertwined Markov chain model as a mean field approximation of the 2^n model via simulation. The proofs of our time-varying results are partially derived from the existing literature on slowly time-varying systems [26]–[31].

This paper is organized as follows. We first introduce our notation. In Section II, we introduce the models from [4] with the mean-field approximation derivation of the n-intertwined Markov chain model from the 2^n-state Markov chain model and present the time-varying extensions of these models. In Section III, we explore the stability properties of the time-varying extensions of the n-intertwined Markov chain model. In Section IV, we evaluate the effectiveness of the mean-field approximations of both the static and time-varying n-intertwined models by comparing them to the 2^n model via simulation. Based on these simulations and others, we state and prove two corollaries. Finally, in Section V, we conclude, summarizing the results and discussing future work.

A. Notation

Given a vector function of time $x(t)$, $\dot{x}(t)$ indicates the time derivative. Given a vector $x \in \mathbb{R}^n$, the 2-norm is denoted by $\|x\|$ and the transpose by x^T. Given two vectors $x_1, x_2 \in \mathbb{R}^n$, $x_1 \leq x_2$ indicates that each element of x_1 is less than or equal to the corresponding element of x_2. Given a matrix $A \in \mathbb{R}^{n\times n}$, the maximum eigenvalue is $\lambda_1(A)$ (if the spectrum is real), and the largest real-valued part of the eigenvalues of A is denoted $s_1(A)$ (if the spectrum is possibly complex). Also, a_{ij} indicates the (i,j)th entry of A, and $\|A\|$ indicates the induced 2-norm of A (the maximum singular value of A). The notation $\mathrm{diag}(\cdot)$ refers to a diagonal matrix with the argument on the diagonal. We use $E[\cdot]$ to denote the expected value of the argument and $Pr[\cdot]$ to denote the probability of the argument.

II. Virus Model

In [4], a 2^n-state Markov chain is introduced, where each state of the chain, $Y_k(t)$, corresponds to a binary-valued vector $x \in \mathbb{R}^n$ and the state transition matrix $\bar{Q}$ is defined by

$$\bar{q}_{kl} = \begin{cases} \delta, & \text{if } x_i = 1, k = l + 2^{i-1} \\ \beta \sum_{j=1}^{n} a_{ij} x_j, & \text{if } x_i = 0, k = l - 2^{i-1} \\ -\sum_{j \neq l} \bar{q}_{jl}, & \text{if } k = l \\ 0, & \text{otherwise} \end{cases} \tag{2}$$

for $i = 1, ..., n$. Here, a virus is propagating over a network structure defined by a_{ij} (nonnegative with $a_{jj} = 0$, $\forall j$), with n agents, β is the infection rate, δ is the healing rate, and $x_i = 1$ or $x_i = 0$ indicates that the ith agent is either infected or susceptible, respectively.

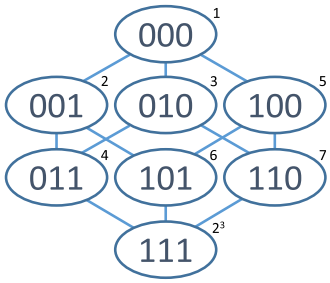

Fig. 1. Example of 2^n-state model with $n = 3$: the superscripts indicate the ordering of the states, which correspond to the subscript of $y_k(t)$ in (3), and the internal strings indicate which agents are healthy (0) and which are infected (1), corresponding to x_i in (2).

The state vector $y(t)$ is defined as

$$y_k(t) = \Pr[Y_k(t) = k] \tag{3}$$

with $\sum_{k=1}^{2^n} y_k(t) = 1$. The Markov chain evolves as

$$\frac{dy^T(t)}{dt} = y^T(t)\bar{Q}. \tag{4}$$

See Fig. 1 for an example of this chain with $n = 3$. Let $v_i(t) = Pr[X_i(t) = 1]$, where $X_i(t)$ is the random variable representing whether the ith agent is infected (not to be confused with x_i, which is the ith entry of the binary string associated with each state of the 2^n Markov chain). Then

$$v^T(t) = y^T(t)M \tag{5}$$

where $M \in \mathbb{R}^{2^n \times n}$ with the rows being lexicographically ordered binary numbers, bit reversed.[1] That is, $v_i(t)$ reflects the summation of all probabilities where $x_i = 1$, therefore giving the mean, $E[X_i]$, of the infection, X_i, of agent i.

A mean-field approximation of this system is used to obtain an n-intertwined continuous Markov chain, where each node has two states: infected with probability $\Pr[X_i(t) = 1]$ and healthy (susceptible) with probability $\Pr[X_i(t) = 0]$. Taking the expected value of the infection transition rate, that is, the second case given in (2), and using $E[1_z] = \Pr[z]$ gives

$$E[\bar{q}_{kl}|x_i = 0, k = l - 2^{i-1}] = E\left[\beta \sum_{l=1}^{n} a_{ij} 1_{\{X_j(t)=1\}}\right] \tag{6}$$

$$= \beta \sum_{l=1}^{n} a_{ij} \Pr[X_j(t) = 1]$$

where the second equality holds since the β and a_{ij} values are deterministic and known.

Denoting $p_i(t) = \Pr[X_i(t) = 1]$ and noting that $\Pr[X_i(t) = 0] = 1 - p_i(t)$, we can see that

$$\dot{p}_i(t) = (1 - p_i(t))\beta \sum_{j=1}^{n} a_{ij} p_j(t) - \delta p_i(t). \tag{7}$$

Applying the central limit theorem, under the assumption of independent indicators, implies that large deviations from the mean are unlikely; this is the motivation for the mean-field approximation. However, it is clear that the indicators are not independent, by construction. The authors of [4] state

$$\Pr[X_j(t) = 1 | X_i(t) = 1] \geq \Pr[X_j(t) = 1]$$

which is true under the assumption $\beta \geq 0$, because if one node in the system is infected, it will have only a nonnegative effect on the probability of infecting other nodes. That is, one agent being infected will never decrease the probability of another agent becoming infected. Therefore, the n-intertwined Markov chain model gives an *upper-bound* for the exact probability, $p_i(t)$, of infection [4]. It has been shown that, under certain conditions, mean-field approximations of SIS models may be inaccurate, leading to incorrect results [32]. However, as we have shown, the mean-field approximation considered herein, while it is an approximation, is well constructed. The shortcomings of this mean-field approximation are illustrated in Section IV.

The model in (7) can be generalized to the heterogeneous virus directed graph structure case:

$$\dot{p}_i(t) = (1 - p_i(t))\beta_i \sum_{j=1}^{n} a_{ij} p_j(t) - \delta_i p_i(t) \tag{8}$$

where β_i is the nonnegative susceptibility or infection rate of agent i, n is the number of agents, a_{ij} reflects the directed, nonnegative, weighted, connection between agents, with $a_{ij} = 0$ if agents i and j are not neighbors, and δ_i is the nonnegative healing rate of agent i. In matrix form, with $p(t)$ representing the vector of the probabilities of infection of the agents, the model is

$$\dot{p}(t) = (BA - P(t)BA - D)p(t) \tag{9}$$

where $B = \text{diag}(\beta_1, \ldots, \beta_n)$, $A = [a_{ij}]$ represents the weighted network structure, $P(t) = \text{diag}(p_1(t), \ldots, p_n(t))$, and $D = \text{diag}(\delta_1, \ldots, \delta_n)$. Each node of the network can be interpreted as an individual agent [4], or as the centroid of a community, i.e., as a grouping of individuals [3]. While using the first interpretation, where p_i is the probability of infection of agent i, allowing a_{ii} to be nonzero can cause problems with the independent indicators assumption. Using the second interpretation, where p_i is the percentage of group i infected, makes nonzero a_{ii} permissible. Therefore, for the analysis in the rest of this paper, we allow this generalization.

In this paper, a time-varying extension of the model in (9) is considered, that is

$$\dot{p}(t) = (BA(t) - P(t)BA(t) - D)p(t) \tag{10}$$

where now $A(t)$ is a function of time. Note that $A(t)$ is not necessarily symmetric and depicts the links between the n agents, similar to an adjacency matrix without the constraint to be binary valued. The mean-field approximation in (6) remains unaffected by this extension as long as the assumption is made that the $a_{ij}(t)$'s are deterministic and known functions. We assume that $p_i(0) \geq 0$ for all $i = 1, ..., n$.

Lemma 1: If $p_i(0) \geq 0$, for all $i = 1, ..., n$, then $p_i(t) \geq 0$ for all $t \geq 0$, $i = 1, ..., n$.

[1]Matlab code: $M = fliplr(dec2bin(0 : (2^n) - 1) - '0')$

Proof: Assume $p_i(0) = 0$ and $p_j(0) \geq 0$ for all $j \neq i$. Then, by (8), $\dot{p}_i(0) \geq 0$, driving $p_i(t) \geq 0$ for $t > 0$.

Assume $p_i(0) > 0$ and $p_j(0) \geq 0$ for all $j \neq i$. Since there exists a derivative by (10), $p_i(t)$ is continuous. Now, suppose $\dot{p}_i(t) < 0$, for some interval $0 \leq \tau \leq t \leq T$, where, by the continuity of $p_i(t)$, at time T we have $p_i(T) = 0$. Then, similar to the first part of the proof, by (8), $\dot{p}_i(T) \geq 0$ and $p_i(t) \geq 0$ for $t > T$. ■

For completeness, we also include a time-varying extension of the model in (4). The extended model is

$$\frac{dy^T(t)}{dt} = y^T(t)\bar{Q}(t) \tag{11}$$

where

$$\bar{q}_{kl}(t) = \begin{cases} \delta, & \text{if } x_i = 1, k = l + 2^{i-1} \\ \beta \sum_{j=1}^{n} a_{ij}(t)x_j, & \text{if } x_i = 0, k = l - 2^{i-1} \\ [2.5ex] - \sum_{j \neq l} \bar{q}_{jl}(t), & \text{if } k = l \\ 0, & \text{otherwise.} \end{cases}$$

Due to the immense size of the 2^n model, it is quite costly to employ, which makes the mean-field approximation useful.

III. Stability Analysis of the Time-Varying Model

In this section, stability analysis of the DFE for the time-varying model in (10) is performed for the deterministic case and several stochastic cases.

A. Deterministic Case

The DFE is the state where $p_i(t) = 0$ for all i, which from (10) implies $\dot{p}_i(t) = 0$ for all i. We show global exponential convergence to the DFE under certain conditions, to be made precise.

1) Undirected Graph and Homogeneous in β Case:

Theorem 1: Suppose $\beta_i = \beta \ \forall i$, $A(t)$ is symmetric, piecewise continuous in t, and bounded, and $\sup_{t \geq 0} \lambda_1(BA(t) - D) < 0$. Then, the DFE is globally exponentially stable (GES).

Proof: To simplify notation, we will write $p = p(t)$. Consider an arbitrary $p \geq 0$ and define a Lyapunov function $V(p) = \frac{1}{2}p^T p$. For $p \neq 0$,

$$\begin{aligned} \dot{V}(p) = p^T \dot{p} &= p^T(BA(t) - P(t)BA(t) - D)p \\ &\leq p^T(BA(t) - D)p \\ &\leq \lambda_1(BA(t) - D)\|p\|^2 \\ &\leq \left(\sup_{t \geq 0} \lambda_1(BA(t) - D)\right)\|p\|^2 < 0. \end{aligned}$$

The first inequality holds because $(P(t)BA(t))_{ij} \geq 0, \ \forall i, j$, $\beta \geq 0, a_{ij} \geq 0$ for all i, j, by assumption, and $p_i(t) \geq 0$ for all i, by Lemma 1. The second inequality holds by the Rayleigh–Ritz Quotient (RRQ) [33] because $BA(t) - D$ is symmetric (since $A = A^T$ and $\beta_i = \beta \ \forall i$). The last inequality holds by definition of the supremum. Therefore, since the system is piecewise continuous in t and, by the boundedness of $A(t)$, locally Lipschitz in $p \ \forall t, p \geq 0$, the system converges exponentially fast to the origin by [34, Th. 8.5]. ■

Remark 1: Theorem 1 requires $BA(t) - D$ to be symmetric because of the chosen Lyapunov function in the proof, which considerably simplifies the analysis. The RRQ cannot be applied unless the matrix under consideration is symmetric, which is not satisfied for BA when the virus is heterogeneous in infection rate. However, note if the Lyapunov function $V(p) = \frac{1}{2}p^T B^{-1}p$ is used, assuming $\beta_i > 0$ for all i, the result of Theorem 1 can be shown in terms of $\lambda_1(A(t) - B^{-1}D)$.

The following lemma and theorem explore the case where symmetry is not assumed, that is, for the heterogeneous model (different β_i's and δ_i's $\forall i$) and asymmetric matrices ($A \neq A^T$).

2) Directed Graph and Heterogeneous Virus Case: The following result and proof are similar to [30, Th. 3.4.11] and the Lyapunov analysis is done pointwise in t.

Definition 1: Assume that for all $t \geq 0$, there exist finite $c(t), \lambda(t) > 0$ such that

$$\|BA(t) - D\| \leq c(t)e^{-\lambda(t)t} \ \ \forall t \geq 0. \tag{12}$$

We then define

$$\begin{aligned} \gamma_1 &:= \sup_{t \geq 0} \int_0^\infty c(t)^2 e^{-2\lambda(t)\tau} d\tau \\ &\geq \left\| \int_0^\infty e^{(BA(t)-D)^T\tau} e^{(BA(t)-D)\tau} d\tau \right\|. \end{aligned} \tag{13}$$

Theorem 2: Consider the system in (10) with $A(t)$ continuously differentiable and $BA(t) - D$ bounded, that is, there exists an $L > 0$ such that $\|BA(t) - D\| \leq L \ \forall t$. Assume that $\sup_{t \geq 0} s_1(BA(t) - D) < 0$, and γ_1 in Definition 1, is well defined and finite. If $\sup_{t \geq 0} \|B\dot{A}(t) - D\| < \frac{1}{2\gamma_1^2}$ or $\int_t^{t+T} \|B\dot{A}(s) - D\|ds \leq \mu T + \alpha$ for small enough $\mu > 0$, then the DFE is GES.

Proof: Note that since $(P(t)BA(t))_{ij} \geq 0 \ \forall i, j$, by construction and Lemma 1,

$$\begin{aligned} \dot{p} &= (BA(t) - P(t)BA(t) - D)p \\ &\leq (BA(t) - D)p. \end{aligned} \tag{14}$$

Therefore, by Grönwall's Inequality (see [35]), the solution of the original system will be bounded above by the solution of the linear system. Stability of the linear time-varying model follows from [26] and [30]; for completeness, we include a clarified version for the virus case.

Since $\sum_{t \geq 0} s_1(BA(t) - D) < 0$, we have $BA(t) - D$ is Hurwitz for all $t \geq 0$, and therefore, for any given $t \geq 0$, (14) is exponentially stable. This also implies that for any given t, there exists a symmetric positive definite $Q(t)$ (by [34, Th. 4.6]) such that

$$Q(t)(BA(t) - D) + (BA(t) - D)^T Q(t) = -I. \tag{15}$$

Note that the solution to this equation is given by

$$Q(t) = \int_0^\infty e^{(BA(t)-D)^T\tau} e^{(BA(t)-D)\tau} d\tau. \tag{16}$$

By our assumption, there exists an $L > 0$ such that $\|BA(t) - D\| \leq L \; \forall t$, which implies for any $\tau > 0$

$$\|p\| \leq e^{L\tau} \left\| e^{(BA(t)-D)\tau} p \right\|.$$

Therefore, $\|e^{(BA(t)-D)\tau} p\| \geq e^{-L\tau} \|p\|$, so from (16), we have

$$p^T Q(t) p \geq \gamma_0 \|p\|^2 \tag{17}$$

where $\gamma_0 := \int_0^\infty e^{-2L\tau} d\tau = \frac{1}{2L}$.

Let $V(p,t) = p^T Q(t) p$. By (13), (16), and (17), we have

$$\gamma_0 \|p\|^2 \leq p^T Q(t) p \leq \gamma_1 \|p\|^2 \tag{18}$$

where γ_1 is well defined and finite by assumption. Taking the time derivative of $V(p,t)$ gives

$$\begin{aligned} \dot{V} &= p^T (Q(t)(BA(t) - D) \\ &\quad + (BA(t) - D)^T Q(t) + \dot{Q}(t)) p \\ &= - \|p\|^2 + p^T \dot{Q}(t) p \end{aligned} \tag{19}$$

where the second equality follows from (15). Taking the time derivative of (15) and rearranging terms gives

$$\begin{aligned} &\dot{Q}(t)(BA(t) - D) + (BA(t) - D)^T \dot{Q}(t) = \\ &- Q(t)(B\dot{A}(t) - D) - (B\dot{A}(t) - D)^T Q(t) =: R(t). \end{aligned} \tag{20}$$

Note

$$\|R(t)\| \leq 2\|Q(t)(B\dot{A}(t) - D)\| \leq 2\|Q(t)\|\|B\dot{A}(t) - D\|. \tag{21}$$

The solution to (20) is

$$\dot{Q}(t) = \int_0^\infty e^{(BA(t)-D)^T \tau} R(t) e^{(BA(t)-D)\tau} d\tau.$$

Therefore

$$\|\dot{Q}(t)\| \leq 2\gamma_1^2 \|B\dot{A}(t) - D\|. \tag{22}$$

Substituting (22) into (19) and using (15) gives

$$\dot{V}(p,t) \leq -(1 - 2\gamma_1^2 \|B\dot{A}(t) - D\|)\|p\|^2. \tag{23}$$

Thus, for $\sup_{t>0} \|B\dot{A}(t) - D\| < \frac{1}{2\gamma_1^2}$, the origin is GES.

Otherwise, using (18), we can rewrite (23) as

$$\dot{V}(p,t) \leq - \left(\frac{1}{\gamma_1} - 2\frac{\gamma_1^2}{\gamma_0} \|B\dot{A}(t) - D\| \right) V(p,t).$$

By the comparison lemma (see, e.g., [34, Sec. 3.4]), we have

$$V(p,t) \leq e^{2\frac{\gamma_1^2}{\gamma_0}\alpha} e^{-\left(\frac{1}{\gamma_1} - 2\frac{\gamma_1^2}{\gamma_0}\mu\right)(t-t_0)} V(p(t_0), t_0).$$

Therefore, since $\int_t^{t+T} \|B\dot{A}(s) - D\| ds \leq \mu T + \alpha$ by our assumption, if $\mu < \frac{\gamma_0}{2\gamma_1^3}$ then, with $\bar{c} = e^{2\frac{\gamma_1^2}{\gamma_0}\alpha}$ and $\bar{\lambda} = \frac{1}{\gamma_1} - 2\frac{\gamma_1^2}{\gamma_0}\mu$,

$$\|p(t)\| \leq \bar{c} e^{-\bar{\lambda}(t-t_0)} \|p(t_0)\|,$$

that is, the origin is GES.

Therefore, by (14), the DFE is GES (in the latter case, for small enough μ) for the system in (10). ■

Next, we consider the case where the linearized system is not always Hurwitz. We first introduce a lemma.

Lemma 2: Consider the system

$$\dot{p} = (BA(t) - D + B\Delta(t))p.$$

Assume

$$\lim_{T\to\infty} \frac{1}{T} \int_{t_0}^{t_0+T} \|BA(s) - D\| ds \leq a < \infty \tag{24}$$

for all $t_0 \geq 0$, and for some $\nu > 0$, there exists an $h > 0$ such that

$$\|BA(t+h) - BA(t)\| \leq \nu h^\gamma \tag{25}$$

for all $t \geq 0$ and some γ, $0 < \gamma \leq 1$. Assume

$$\lim_{T\to\infty} \frac{1}{T} \int_{t_0}^{t_0+T} s_1(BA(s) - D) ds \leq \bar{\alpha} \tag{26}$$

for some negative scalar $\bar{\alpha}$ and for all $t_0 \geq 0$, and

$$\lim_{T\to\infty} \frac{1}{T} \int_{t_0}^{t_0+T} \|B\Delta(s)\| ds \leq \eta < \infty \tag{27}$$

for all $t_0 \geq 0$. Then, the DFE is exponentially stable.

Lemma 2 is a direct application of [31, Th. 2].

Theorem 3: Consider

$$\dot{p} = (B(A(t) + \Delta(t)) - P(t)B(A(t) + \Delta(t)) - D)p.$$

Assume (24)–(27) hold, and $\forall i, j$ and $t \geq 0$, the perturbation

$$|\Delta_{ij}(t)| \leq a_{ij}(t). \tag{28}$$

Then, the DFE is exponentially stable.

Proof: Since $(P(t)B(A(t) + \Delta(t)))_{ij} \geq 0 \; \forall i, j$ by (28) and Lemma 1,

$$\begin{aligned} \dot{p} &= (B(A(t) + \Delta(t)) - P(t)B(A(t) + \Delta(t)) - D)p \\ &\leq (B(A(t) + \Delta(t)) - D)p. \end{aligned}$$

Therefore, by Grönwall's inequality (see [35]), the solution of the original system will be bounded above by the solution of the linear system. Thus, by Lemma 2, the DFE for the system in (29) is exponentially stable. ■

Remark 2: In the context of disease propagation, these results tell us that the infection rates, β_i, can dominate the healing rates, δ_i, and nevertheless, if the interactions between the agents have certain behavior, the virus can still be eradicated.

Note that the assumption in (24) states that the unperturbed linearized system cannot get too large on average. In the context of virus spread, this means that the element values of the matrix $A(t)$ combined with the corresponding infection rates cannot get too large with respect to the corresponding healing rate, on average. The assumption in (25) is a uniform Lipschitz condition and states that the agents' interactions cannot change too quickly. The assumption in (26) imposes that the time average of the unperturbed linearized system is Hurwitz. We will see that this result is supported by the simulations in Section IV. Also, the assumption in (27) states that the perturbation $B\Delta(t)$ cannot be too large, on average.

B. Stochastic Models

In this section, we explore introducing randomness using two different models: a generic additive noise model and an Ito's formula-type model. Note that the mean-field step in (6), in essence, removes the randomness that was included in the original 2^n model. Therefore, an exploration of random graph structures, while interesting as an extension of the n-intertwined Markov model in (10), does not accurately approximate the 2^n model with random graph structure. Alternatively, in this section, we consider the measurement of the virus probabilities to be corrupted with additive noise, which allows for a greater range of potential behaviors to be evaluated. Also, this approach acknowledges that the underlying model is stochastic, without necessitating the high dimensionality of the 2^n state model.

1) Generic Noise: Consider the system

$$\dot{p}(t) = \underbrace{(BA(t) - P(t)BA(t) - D)p(t)}_{F(t,p)} + g(t,p)\xi(t,\omega) \quad (29)$$

which represents a perturbation to the model in (10), where $\xi(t,\omega) \in \mathbb{R}^k$ is a zero mean measurable stochastic process, $A(t)$, B, D, and $g(t,p)$ are deterministic, $g(t,p) \in \mathbb{R}^{n\times k}$, and $g(t,0) = 0$ for all t. We assume that $p_i(0) \geq 0$ for all $i = 1, ..., n$.

Lemma 3: Consider the system in (29) with $p_i(0) \geq 0$, for all $i = 1, ..., n$. If $\xi(t,\omega) \in \mathbb{R}^k$ is a zero mean measurable stochastic process and, for all $i = 1, ..., n$, there exists a $k_i > 0$ such that $\|g_i(t,p)\| \leq k_i|p_i|^2$ for all $t \geq 0$, then $p_i(t) \geq 0$ for all $t \geq 0$, $i = 1, ..., n$.

Proof: By Lemma 1, the deterministic part of (29), $F(t,p)$, is nonnegative for all $t \geq 0$. Therefore, we turn our attention to the $g_i(t,p)\xi(t,\omega)$ term, where i refers to the ith row of $g(t,p)$. By the zero mean and independence assumptions, $\xi(t,\omega)$ can be negative for any $t \geq 0$. However, by our assumption that $\|g_i(t,p)\| \leq k_i|p_i|^2$ for all t, we have , for any $t \geq 0$,

$$\lim_{p_i\to 0} \|g_i(t,p)\xi(t,\omega)\| \leq \lim_{p_i\to 0} \|g_i(t,p)\|\|\xi(t,\omega)\| \leq \lim_{p_i\to 0} k_i|p_i|^2\|\xi(t,\omega)\| = 0.$$

Therefore, if $p_i(0) \geq 0$, then as p_i approaches zero, the random part of the derivative vanishes. Therefore, if $p_i(t) = 0$, then $\dot{p}_i(t) \geq 0$, and consequently, $p_i(t) \geq 0$ for all $t \geq 0$. ■

We have the following result.

Theorem 4: Consider the system in (29) with $\beta_i = \beta\ \forall i$, $A(t)$ symmetric, piecewise continuous in t, and bounded, and $\sup_{t\geq 0} \lambda_1(BA(t) - D) < 0$. If $\xi(t,\omega) \in \mathbb{R}^k$ is a zero mean measurable stochastic process and, for all $i = 1, ..., n$, there exists a $k_i > 0$ such that $\|g_i(t,p)\| \leq k_i|p_i|^2$ for all $t \geq 0$, then the DFE is GES in expectation.

Proof: Consider an arbitrary p and define a Lyapunov function $V(p) = \frac{1}{2}p^T p$. For $p \neq 0$,

$$\begin{aligned} E[\dot{V}(p)|p] &= E[p^T\dot{p}|p] \\ &= p^T(BA(t) - P(t)BA(t) - D)p \\ &\quad + p^T g(t,p)E[\xi(t,\omega)] \quad (30) \\ &= p^T(BA(t) - P(t)BA(t) - D)p \quad (31) \\ &\leq p^T(BA(t) - D)p \quad (32) \\ &\leq \lambda_1(BA(t) - D)\|p\|^2 \\ &\leq \left(\sup_{t\geq 0} \lambda_1(BA(t) - D)\right)\|p\|^2 < 0 \end{aligned}$$

where (30) and (31) hold because, by assumption, $E[\xi(t,\omega)|p] = E[\xi(t,\omega)] = 0$, and (32) holds by our assumption that $p_i(0) \geq 0$ for all $i = 1, ..., n$, and by Lemma 3. Thus, since the system is piecewise continuous in t and locally Lipschitz in $p\ \forall t, p \geq 0$, the dynamics converges exponentially fast to the origin by [34, Th. 8.5] in expectation. ■

Remark 3: The assumption that for each $i = 1, ..., n$, there exists a $k_i > 0$ such that $\|g_i(t,p)\| \leq k_i|p_i|^2$ for all $t \geq 0$, may appear to be strong. However, consider the case where $g(t,p)$ is monotonic in p. An explicit real-life example could be the germs of the ith agent spreading to objects in its surroundings as a source of the noise. As agent i becomes healthy, this noise reduces to zero.

We will use the result stated in Lemma 4, from [36], to prove Theorem 5. Note that d^0V/dt is defined as

$$\frac{d^0V}{dt} := \frac{\partial V}{\partial t} + \sum_{i=1}^{n} \frac{\partial V}{\partial p_i} F_i(t,p) \quad (33)$$

where $F_i(t,p)$ is the ith entry of $F(t,p)$ as defined in (29).

Lemma 4 (see [36, Th. 1.12]): Consider the system (29) with a Lyapunov function $V(p,t)$ that is positive definite uniformly in t and $V(0,t) = 0$. If $\xi(t,\omega)$ satisfies the strong law of large numbers

$$\sup_{t\geq 0} E|\xi(t,\omega)| < \frac{c_1}{bc_2} \quad (34)$$

$$\frac{d^0V}{dt} \leq -c_1 V, \text{ and } \|g\| \leq c_2 V \quad (35)$$

for some constants $c_1, c_2, b > 0$, then the origin is almost surely asymptotically stable.

Theorem 5: Consider the system in (29) with $\beta_i = \beta\ \forall i$, $A(t)$ symmetric, and $\sup_{t\geq 0} \lambda_1(BA(t) - D) < 0$. If $\xi(t,\omega)$ is a zero mean, independent and identically distributed (i.i.d.), measurable stochastic process, and for all $i = 1, ..., n$, there exists a $k_i > 0$ such that $\|g_i(t,p)\| \leq k_i|p_i|^2$ for all $t \geq 0$, then the origin is almost surely asymptotically stable.

Proof: Consider the Lyapunov function candidate $V(p) = \frac{1}{2}p^T p$. Clearly, V is positive definite uniformly in t. Since $\sup_{t\geq 0} \lambda_1(BA(t) - D) < 0$, there exists $\varepsilon > 0$ such that for all $t \geq 0$, $\sup_{t\geq 0} \lambda_1(BA(t) - D) \leq -\varepsilon$. Therefore, for $p \geq 0$,

$$\begin{aligned} \frac{d^0V}{dt} &= p^T(BA(t) - P(t)BA(t) - D)p \\ &\leq p^T(BA(t) - D)p \\ &\leq \left(\sup_{t\geq 0} \lambda_1(BA(t) - D)\right)\|p\|^2 \\ &\leq -\varepsilon p^T p = -2\varepsilon V \quad (36) \end{aligned}$$

where (36) follows from our assumption that $p_i(0) \geq 0$ for all $i = 1, ..., n$ and by Lemma 3.

By our assumption $\|g_i(t,p)\| \leq k_i|p_i|^2$, we have that

$$\|g(t,p)\|^2 \leq \sum_{i=1}^{n} \|g_i(t,p)\|^2 \tag{37}$$

$$\leq \sum_{i=1}^{n} (k_i|p_i|^2)^2 \leq c\sum_{i=1}^{n} (|p_i|^2)^2$$

$$\leq c\left(\sum_{i=1}^{n} |p_i|^2\right)^2 \tag{38}$$

$$\leq c\|p\|^4 \tag{39}$$

for all $t \geq 0$, where $c = \max_i k_i^2$. Note (37) holds by the relationship between the 2-induced norm and the Frobenius norm and (38) holds because the cross terms $|p_i|^2|p_j|^2 \geq 0$. Therefore, $\|g(t,p)\| \leq \sqrt{c}V$, so (35) is satisfied. Also, since $\xi(t,\omega)$ is i.i.d., it satisfies the strong law of large numbers and (34) is satisfied by the zero mean assumption. Therefore, by Lemma 4, the origin is almost surely asymptotically stable. ■

A similar result can be shown for the case of asymmetric $A(t)$. Note that here the graph can still be undirected, we just do not require symmetric $A(t)$.

Theorem 6: Consider the system in (29) with $A(t)$ continuously differentiable and $BA(t) - D$ bounded, that is, there exists an $L > 0$ such that $\|BA(t) - D\| \leq L\ \forall t$. Further suppose $\xi(t,\omega)$ are zero mean and i.i.d., and for all $i = 1, ..., n$, there exists a $k_i > 0$ such that $\|g_i(t,p)\| \leq k_i|p_i|^2$ for all $t \geq 0$. Assume that $\sup_{t\geq 0} s_1(BA(t) - D) < 0$, and γ_1 in Definition 1 is well defined and finite. If $\sup_{t\geq 0} \|B\dot{A}(t) - D\| < \frac{1}{2\gamma_1^2}$ or $\int_t^{t+T} \|B\dot{A}(s) - D\|ds \leq \mu T + \alpha$ for small enough $\mu > 0$, then the origin is almost surely asymptotically stable.

Proof: Similar to the proof of Theorems 2 and 5, it can be shown $\frac{d^0V}{dt} \leq -c_1V$.

By our assumption $\|g_i(t,p)\| \leq k_i|p_i|^2$ and (37)–(39), we have that $\|g(t,p)\| \leq \sqrt{c}V$ for all $t \geq 0$, where $c = n(\max_i k_i^2)$. Also, since $\xi(t,\omega)$ is i.i.d., it satisfies the strong law of large numbers and (34) is satisfied by the zero mean assumption. Therefore, by Lemma 4, the origin is almost surely asymptotically stable. ■

2) Ito's Formula-Based Modeling: Consider the system

$$dp(t) = \underbrace{(BA(t) - P(t)BA(t) - D)p(t)dt}_{F(t,p)} + g(t,p)dw \tag{40}$$

which represents a perturbation to the model in (10), where w is a d-dimensional vector of independent standard Wiener processes and $A(t)$, B, D, and $g(t,p)$ are deterministic. Again, assume that $g(t,0) = 0$ for all t, and $p_i(0) \geq 0$ for all $i = 1, ..., n$.

Similar to Lemmas 1 and 3, we can state a positivity result for $p(t)$ in (40).

Lemma 5: Consider the system in (40) with $p_i(0) \geq 0$ for all $i = 1, ..., n$. If, for all $i = 1, ..., n$, there exists a $k_i > 0$ such that $\|g_i(t,p)\| \leq k_i|p_i|$ for all $t \geq 0$, then $p_i(t) \geq 0$ for all $t \geq 0$, $i = 1, ..., n$.

Proof: By Lemma 1, the deterministic part of (40), $F(t,p)$, is nonnegative for all $t \geq 0$. Therefore, we turn our attention to the $g_i(t,p)\xi(t,\omega)$ term, where i refers to the ith row of $g(t,p)$. By our assumption that $\|g_i(t,p)\| \leq k_i|p_i|$, we have , for any $t \geq 0$,

$$\lim_{p_i\to 0} \|g_i(t,p)dw\| \leq \lim_{p_i\to 0} \|g_i(t,p)\|\|dw\|$$

$$\leq \lim_{p_i\to 0} k_i|p_i|\|dw\| = 0.$$

Therefore, if $p_i(0) \geq 0$, then as p_i approaches zero, the random part of the derivative vanishes. Furthermore, if $p_i(t) = 0$, then $\dot{p}_i(t) \geq 0$, and consequently, $p_i(t) \geq 0$ for all $t \geq 0$. ■

We now call several results from [36] in order to develop a result analogous to Theorem 1 for the stochastic model in (40). Consider the system

$$dp = b(t,p)dt + \sum_{r=1}^{k} \sigma_r(t,p)dw_r(t) \tag{41}$$

where w_i's are independent standard Wiener processes and $p(t)$, $b(t,p)$, and $\sigma_r(t,p)$ are vectors in $\mathbb{R}^d$. The *generator operator* (see [36, Ch. 5]), which generalizes the operation of differentiating a Lyapunov function V, is given by

$$\mathcal{L} = \frac{\partial}{\partial t} + \langle b, \frac{\partial}{\partial p}\rangle + \sum_r \langle \sigma_r, \frac{\partial}{\partial p}\rangle^2 \tag{42}$$

where $\langle\cdot,\cdot\rangle$ is the inner product and $\frac{\partial}{\partial p} = \left[\frac{\partial}{\partial p_1}, \ldots, \frac{\partial}{\partial p_n}\right]^T$.

Definition 2 (see [36, Sec. 5.7]): A system is *exponentially 2-stable* if for some constants a, b, and $\forall t \geq 0$,

$$E\|p(t)\|^2 \leq a\|p(0)\|^2 e^{bt}.$$

Theorem 7 (see [36, Ths. 5.11, 15, Sec. 5.7]): Given a system as in (41), if there exists a, twice continuously differentiable with respect to p and continuously differentiable with respect to t, Lyapunov function $V(t,p)$ such that

$$k_1\|p\|^2 \leq V(t,p) \leq k_2\|p\|^2 \tag{43}$$

$$\mathcal{L}V(t,p) \leq -k_3\|p\|^2 \tag{44}$$

for some positive constants k_1, k_2, k_3, then the origin is exponentially 2-stable. Furthermore, the origin is almost surely exponentially stable.

Theorem 8: Consider the system in (40) with $g(t,p)$ bounded and locally Lipschitz in p(t) uniformly in t, w are independent standard Wiener processes, and for all $i = 1, ..., n$, there exists a $k_i > 0$ such that $\|g_i(t,p)\| \leq k_i|p_i|$ for all $t \geq 0$. If $\beta_i = \beta\ \forall i$, $A(t)$ is symmetric, piecewise continuous in t, and bounded, and $\sup_{t\geq 0} \lambda_1(BA(t) - D) < -c$, with $c := \sum_{i=1}^{n} k_i^2 + \epsilon$, $\epsilon > 0$, then the origin is exponentially 2-stable and almost surely exponentially stable.

Proof: Consider the Lyapunov function candidate $V(p) = \frac{1}{2}p^Tp$. Clearly, (43) is satisfied. Since $\frac{\partial V}{\partial p} = \nabla V = p$ and

$\nabla^2 V = I$, we have

$$\begin{aligned}\mathcal{L}V(p) &= \langle b(t,p), \frac{\partial V}{\partial p}\rangle + \langle g(t,p), \frac{\partial V}{\partial p}\rangle^2 \\ &= p^T b(t,p) + \frac{1}{2}\sum_{i,j}(g(t,p)g^T(t,p))_{ij}\frac{\partial V}{\partial p_i \partial p_j} \\ &= p^T(BA(t) - PBA(t) - D)p + \frac{1}{2}\sum_{i=1}^{n} g_i(t,p)g_i^T(t,p) \\ &\leq p^T(BA(t) - D)p + \frac{1}{2}\sum_{i=1}^{n}(k_i|p_i|)^2 \qquad (45) \\ &\leq \left(\sup_{t\geq 0}\lambda_1(BA(t) - D) + \frac{1}{2}\sum_{i=1}^{n} k_i^2\right)\|p\|^2 \qquad (46) \\ &< \left(-c + \frac{1}{2}\sum_{i=1}^{n} k_i^2\right)\|p\|^2 \\ &= -\epsilon\|p\|^2 \qquad (47)\end{aligned}$$

where (45) holds because $PBA(t) \geq 0$, by construction and Lemma 5 and $\|g_i(t,p)\| \leq k_i|p_i|$, for all i, by assumption; (46) holds by the symmetry of $BA(t)$; and (47) holds by definition of c. Thus, (44) is satisfied, and therefore, by Theorem 7, the origin is exponentially 2-stable and almost surely exponentially stable. ■

Remark 4: Note that the results in Theorems 2 and 3 could similarly be extended to the models in (29) and (40).

IV. Simulations and Extensions

In this section, we first compare via simulations the 2^n state and n-intertwined Markov chain models in (4) and (7), respectively, over different graph structures, and then compare them for the complete fully connected graph with the original model in (1). We also provide a comparison of the time-varying graph structure extensions of the analogous time-varying models in (10) and (11). A variety of time-varying simulations are presented, leading to a series of corollaries and observations. Since the infection rate $p(t)$ and the location of the states, $z(t)$, are both time dependent, the simulations are best viewed in video format with links provided in the captions of the figures.

A. Comparison: n-Intertwined and 2^n Markov Chain Models

An initial analysis has been completed in [4] to evaluate the accuracy of the mean-field approximation used in the derivation of the n-intertwined model in (7). This analysis was performed only for the complete graph for $n = 11$ with three (β, δ) pairs. We further the analysis here by including additional graph structures (see Fig. 2), values of n, (β, δ) combinations, and different initial conditions. Simulations include static and dynamic cases, for both the n-intertwined and the 2^n models.

1) Static Graphs: The static graph structures considered in the simulations are line graphs, star (hub–spoke) graphs, and complete graphs; see Fig. 2 for examples of each graph structure. All A matrices for these graphs are symmetric and binary valued. In the star graph, the central node is the first agent. Each simulation was run for 10 000 time steps (final time $T = 10\,000$), with three initial conditions: 1) every agent infected, $p^1(0) = [1 \ \cdots \ 1]^T$; 2) half the agents infected, $p^2(0) = [1 \ \cdots \ 1 \ 0 \ \cdots \ 0]^T$; and 3) one agent infected, $p^3(0) = [1 \ 0 \ \cdots \ 0]^T$. We explore the homogeneous virus case in these tests. The (β, δ) pairs used are $[(.1,1),(.215,1),(.464,1),(.5,.5),(1,.464),(1,.215),(1,.1)]$, and the number of agents, $n = 6, 8, 10, 12$. We limited simulations to these n values since mean-field approximations are typically worse for small values of n, and there is a computational limitation due to the size of the 2^n model.

The results are given in Figs. 3–5 in terms of the 2-norm of the difference between the state of the n-intertwined Markov chain model at the final time $(p(T))$, and the mean of the 2^n Markov model at the final time $(v(T)$ as defined by (5)). Since the n-intertwined Markov chain model is an upper bounding approximation, the results show that the two models converge to the DFE for most of the values of $\frac{\beta}{\delta}$ close to $1/10$, resulting in small errors. For most of the values of $\frac{\beta}{\delta}$ near 10, the n-intertwined Markov chain model again performs quite well since

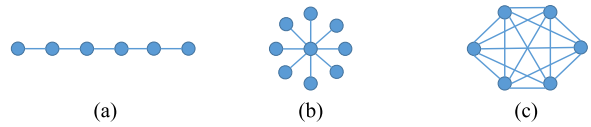

Fig. 2. Graph structures. (a) Line. (b) Star. (c) Complete.

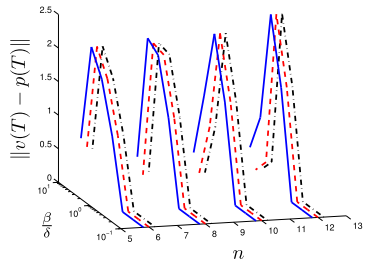

Fig. 3. Plot of $\|v(T) - p(T)\|$ for the line graph, $T = 10\,000$. Results from using the different initial conditions $p^1(0)$, $p^2(0)$, and $p^3(0)$ are depicted by the blue lines, red dashed lines, and black dashed-dotted lines, respectively. For a simulation of $n = 6$, $\frac{\beta}{\delta} = 1$, and $p(0) = p^3(0)$, see youtu.be/E49OTI4Pgh0.

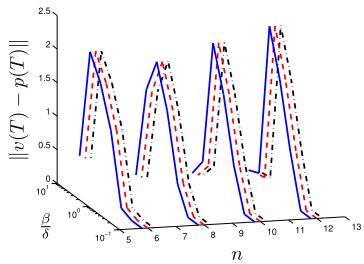

Fig. 4. Plot of $\|v(T) - p(T)\|$ for the star graph, $T = 10\,000$. Results from using the different initial conditions $p^1(0)$, $p^2(0)$, and $p^3(0)$ are depicted by the blue lines, red dashed lines, and black dashed-dotted lines, respectively. For a simulation of $n = 6$, $\frac{\beta}{\delta} = 1$, and $p(0) = p^3(0)$, see youtu.be/XOdNUDFngO4.

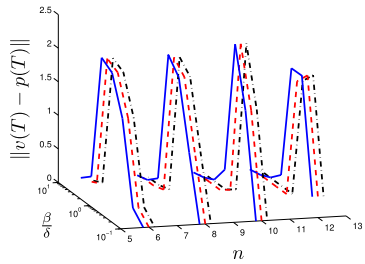

Fig. 5. Plot of $\|v(T) - p(T)\|$ for the full graph, $T = 10\,000$. Results from using the different initial conditions $p^1(0)$, $p^2(0)$, and $p^3(0)$ are depicted by the blue lines, red dashed lines, and black dashed-dotted lines, respectively. For a simulation of $n = 6$, $\frac{\beta}{\delta} = 1$, and $p^3(0)$, see youtu.be/VTFZDdXsC6M.

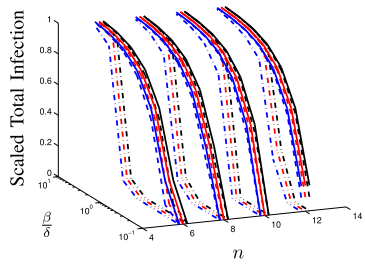

Fig. 6. Comparison of complete graph models to (1): The plots of $\frac{1}{n}I(T)$, $\frac{1}{n}\sum_{i=1}^{n} p_i(T)$, $\frac{1}{n}\sum_{i=1}^{2^n} v_i(T)$ with $T = 10\,000$ are shown in solid, dashed, and dashed-dotted lines, respectively. Results from using the different initial conditions $p^1(0)$, $p^2(0)$, and $p^3(0)$ are shown in blue, red, and black, respectively.

it is at an NDFE and the 2^n state model does not appear to reach the DFE in finite time. Therefore, for certain time scales, the n-intertwined model approximation could be sufficient. For values of $\frac{\beta}{\delta}$ that are not near $1/10$ or 10, the models differ quite drastically; the n-intertwined Markov chain model appears to be at an NDFE, while the 2^n model appears, in most of the cases, to be at or close to the DFE, resulting in large errors.

2) Complete Graphs: For completeness, we present a comparison of the results from the static complete graph to the results of simulating the original model in (1). Since (1) models the population as two groups, we take the average infection of the results of the n-intertwined model ($\frac{1}{n}\sum_{i=1}^{n} p_i(T)$) and the means of the 2^n model [$\frac{1}{n}\sum_{i=1}^{n} v_i(T)$, with $v(t)$ defined in (5)]. These averages, with the scaled results of (1) ($\frac{1}{n}I(T)$), are compared in Fig. 6. Note that the initial conditions $p^1(0)$, $p^2(0)$, and $p^3(0)$ are analogous to $I^1(0) = n$, $I^2(0) = n/2$, and $I^3(0) = 1$, respectively. All three models behave similarly at the extremes and the original and n-intertwined models [in (1) and (7)] perform closely for all of the (β, δ) pairs. The 2^n model differs in most of the mid-valued ranges of $\frac{\beta}{\delta}$, which is consistent with Fig. 5 and with the upper-bounding effect of the n-intertwined model.

3) Dynamic Graphs: In this section, we use several examples to highlight the effectiveness and ineffectiveness of the n-intertwined model in (10) as a mean-field approximation of (11) for dynamic graph structures. For these simulations, the

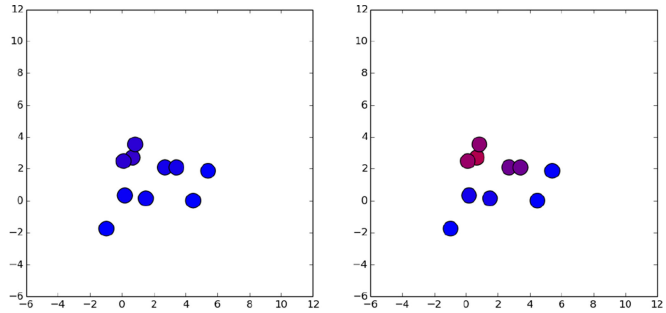

Fig. 7. This system has constant drift as given by (49) for each node with $r = 1$. The 2^n model is on the left and the n-intertwined model is on the right. Blue indicates the agent is healthy and red indicates the agent is infected. This figure gives a snapshot of the system at time 40. For a video of this simulation, see youtu.be/-LmPj7oynLs.

weighting matrix $A(t)$ is dependent on the agents' relative positions, that is, using the definition from [37], for some radius r and $i \neq j$,

$$a_{ij}(t) = \begin{cases} e^{-\|z_i(t) - z_j(t)\|^2}, & \text{if } \|z_i(t) - z_j(t)\| < r \\ 0, & \text{otherwise} \end{cases} \tag{48}$$

where $z_i(t) \in \mathbb{R}^d$ is the position of agent i in d-space. Note that under the construction in (48), $A(t)$ is symmetric.

First, consider the case of constant drift for the positional dynamics of the agents, that is,

$$\dot{z}(t) = \phi \tag{49}$$

where ϕ is some constant vector. As we see in Fig. 7, the upper bounding nature of the n-intertwined Markov chain model leads to a decent approximation; at time step 40, the 2^n model has reached the DFE, whereas the n-intertwined Markov chain model has not. However, the n-intertwined model reaches the DFE shortly thereafter (see the link referenced in the caption of Fig. 7).

For another comparison, we will use a piecewise constant drift so that the agents remain confined to a fixed region. Without loss of generality, let the constrained region be a hypercube l^d, where d is the dimension of the space, centered at some point z_c. That is, the dynamics follow (49), but instead of a constant ϕ term for each agent, we have

$$\phi_k = \begin{cases} -\phi_k, & \text{if } z_k = z_{c_k} + l/2 \text{ or } z_k = z_{c_k} - l/2 \\ \phi_k, & \text{otherwise} \end{cases} \tag{50}$$

for each dimension $k = 1, \ldots, d$. That is, if an agent hits a boundary, the velocity of the agent in the dimension corresponding to that boundary flips sign. As illustrated in Fig. 8, the upper bounding nature of the n-intertwined Markov chain model leads to an inaccurate approximation, as the 2^n model reaches the DFE, but the n-intertwined model does not and does not appear to be tending toward the DFE.

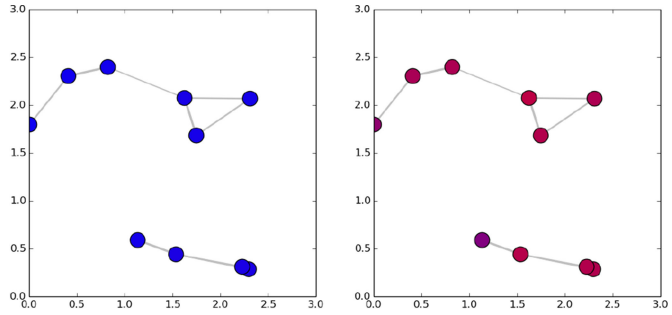

Fig. 8. This system has piecewise constant drift as given by (50) for each node with $r = 1.5$. The 2^n model is on the left and the n-intertwined model is on the right. Blue indicates the agent is healthy and red indicates the agent is infected. This figure gives a snapshot of the system at time 40. For a video of this simulation, see youtu.be/BMn4FGnBZX0.

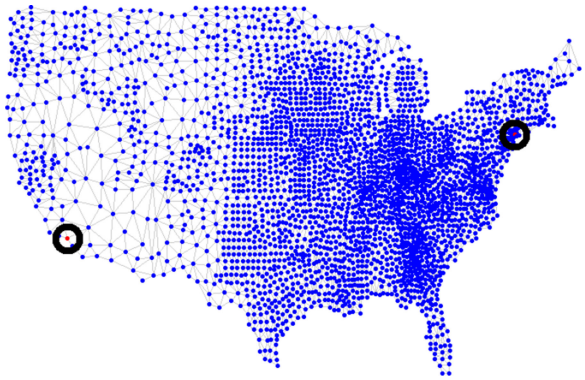

Fig. 9. Initial condition with the virus originating from New York City and Los Angeles, indicated in red and circled to highlight their locations. The average infection proportion is $\frac{2}{3109}$.

B. Exploratory Large-Scale Data and Time-Varying Networks and Extensions

Considering large-scale data networks and different dynamics models provides us with several insights which we state in two corollaries to Theorem 1.

1) Virus Spread Over a Large-Scale Dataset: To illustrate the behavior of these systems, we simulate the evolution of a virus process over a network representing the United States of America. We assume the virus starts in New York City and Los Angeles (see Fig. 9). The nodes of the graph correspond to counties in the domestic United States and are placed in the centroid of each county. The edges denote that two counties are adjacent, with the corresponding A matrix being symmetric with ones on the diagonal. The off-diagonals of the A matrix are equal to 100 times the inverse of the 2-norm distance between the centroids (given in latitude and longitude). We recognize that the homogeneity in the edge construction (opposed to heavier connections between more frequented edges) is probably not the most realistic, but it still provides an effective illustration. The infection rate corresponds to the percentage of the county infected, or alternatively, the probability the county is infected. We simulated two homogeneous viruses with $(\beta_1, \delta_1) = (.1, .1)$ and $(\beta_2, \delta_2) = (.1, .22)$. The steady states of the two viruses can be seen in Figs. 11 and 12, and Fig. 10 shows an intermediate state.

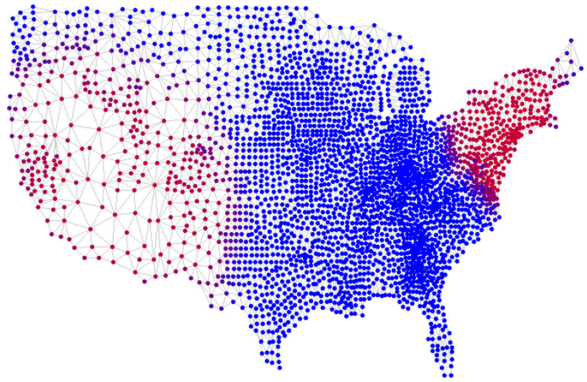

Fig. 10. Virus $(\beta_1, \delta_1) = (.1, .1)$ after 45 time steps of propagating. The average infection proportion is 0.1561.

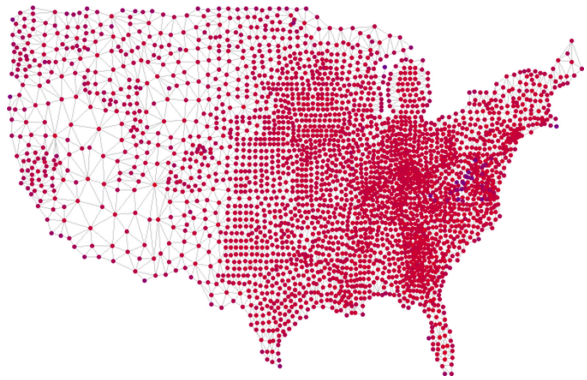

Fig. 11. NDFE equilibrium of the virus $(\beta_1, \delta_1) = (.1, .1)$. The average infection proportion is 0.7586.

Fig. 12. NDFE equilibrium of the virus $(\beta_2, \delta_2) = (.1, .22)$. The average infection proportion is 0.6904.

2) Constant Drift: If the agents have constant (nonequal) drift, as defined in (49), they will eventually float away from each other far enough that, assuming they have nonzero healing rate, the disease will be eradicated. This is illustrated in the simulations depicted in Fig. 7.

This behavior is captured in the following corollary.

Corollary 1: If $B = \beta I$ and $A(t)$ is symmetric, piecewise continuous in t, and bounded $\forall t \geq T$, and for some fixed T, $\sup_{t \geq T} \lambda_1(BA(t) - D) < 0$, then $\forall t \geq T$, the DFE is GES.

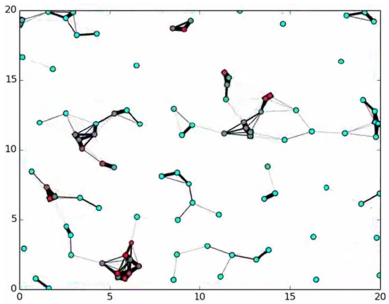

Fig. 13. This system has 100 agents with random initial conditions and piecewise constant drift as explained in (50) for each node with $r = 3$. Teal indicates the agent is healthy and red indicates the agent is infected. This figure gives a snapshot of the system. For a video of this simulation, see youtu.be/Q05TPES5VNU.

Proof: Let $\hat{t} = t - T$. The result follows immediately from applying Theorem 1 to $\dot{p}(\hat{t})$ for $\hat{t} \geq 0$. ■

3) Piecewise Constant Drift: Consider the n-intertwined model with piecewise constant drift illustrated in Fig. 13. At several time instances, the disease appears to be approaching the DFE, but when the graph structure changes, due to agents coming into close proximity of each other, the system is pushed away from the DFE.

C. Quarantine

If the system is too dense, then the agents can be partitioned into distinct groups, spatially bounding them to separate regions. This technique is called a quarantine [38], [39] and is reflected in the model by removing edges in the graph, i.e., setting specific elements of the A matrix to zero. The quarantine essentially imposes a block diagonal structure on the A matrix, given that the states are properly ordered; this restricts interaction between certain agents, which can clearly reduce the spread of a virus.

A quarantine is difficult to implement, as was witnessed recently with the Ebola virus [40]. A quarantine could also be effected by less costly implementations, such as, decreasing human contact via limiting handshakes and other greetings, instilling good habits of covering mouths, etc. Without restricting movement, these measures would decrease the weight of the links between agents, which would be reflected in the model by decreasing the values of a_{ij}.

For the following discussion, we assume that A is symmetric. If the a_{ij}'s can be restricted such that, for $\epsilon_i < 0$,

$$\sup_{t \geq 0} \sum_{i=1}^{n} a_{ij}(t) \leq \epsilon_i + \frac{\delta_i}{\beta} \quad \forall i$$

$$\Rightarrow \beta \sup_{t \geq 0} \sum_{i=1}^{n} a_{ij}(t) - \delta_i \leq \epsilon_i \quad \forall i.$$

Therefore, under the above assumption,

$$\sup_{t \geq 0} \lambda_1(BA(t) - D) < 0$$

by the Gershgorin Disc theorem [33]. Therefore, by Theorem 1, the disease will be eradicated in exponential time.

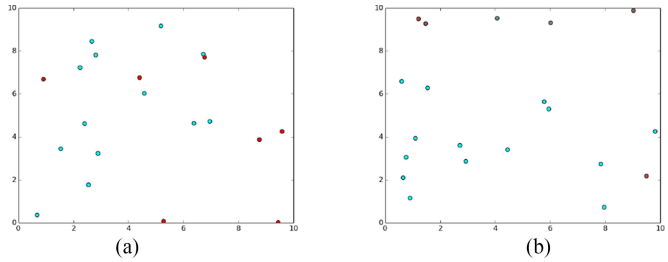

Fig. 14. This system has piecewise constant drift as explained in (50) for each node and evolves for 400 time steps. After 50 time steps, a quarantine is implemented, limiting the agents to certain regions. This separates the sick and those more prone to get sick from the other agents. For a video of this simulation, see youtu.be/NfskXS83FHI. (a) System at time zero. (b) System at time 400.

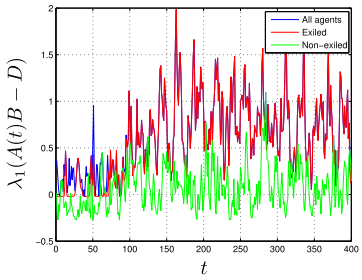

Fig. 15. Maximum eigenvalues of the system shown in Fig. 14 are plotted versus time. The blue line is the total system, the red line is the outside (sick) group, and the green line is the inside (healthy) group. Notice the max eigenvalue of the inside group is below zero on average.

We can implement a quarantine on the piecewise constant drift case by imposing a block diagonal structure, limiting the movement of certain agents so that they do not interact with others. Consider a system with 20 agents, originally confined to a 40×40 box with certain random initial conditions [see Fig. 14(a)]. After 50 time steps, a quarantine is imposed, limiting some agents to the region $[0, 25] \times [0, 25]$ and exiling the rest of the agents to the outside boundary. This separates the sick and the more prone to get sick agents from the others. One set of agents is tending toward the DFE and the other is not, which is consistent with the maximum eigenvalue plot in Fig. 15. Note that the behavior of the maximum eigenvalue of the non-exiled group is consistent with Theorem 3, that is, the average is less than zero. This simulation leads to the following corollary:

Corollary 2: Imposing a block diagonal graph structure, such that $A(t) = diag(A_1(t), \ldots, A_q(t))$, makes the DFE GES if $\lambda_1(B_l A_l(t) - D_l) < 0$ for all $t \geq 0$ and $l = 1, \ldots, q$, with $B_l = \beta_l I$ and $A(t)$ symmetric, piecewise continuous in t, and bounded $\forall t \geq 0$.

Proof: Since $A(t)$ is block diagonal and B and D are diagonal, $p(t)$ can be partitioned into q groups. Then, the result follows immediately from applying Theorem 1 to each $\dot{p}_l(t)$. ■

This approach does not consider any reintegration process for healed agents. For this to be a feasible effective control technique, healed agents would have to be allowed to rejoin the general population. Therefore, an agent by agent policy could be implemented so that once an agent was healed, i.e., $p_i(t) = 0$ for

some t, readmittance would be permitted, contingent on them remaining healthy during re-entrance.

V. Conclusion

We have extended well-studied SIS models to the time-varying graph structure case and considered additive stochastic uncertainty. Prior to this, the dynamic modeling of such systems has mainly focused on networks with static graph structures. This extension makes the models more realistic and provides advanced insights into disease propagation in a greater variety of settings. Stability analyses of the time-varying, weighted, undirected and directed, deterministic, and stochastic n-intertwined Markov chain models for the DFE are provided. Previous work has required the linearized system to be strictly Hurwitz for guaranteed stability of the DFE; in Theorem 3, we provide a relaxation of this assumption.

We compare the 2^n model and the n-intertwined Markov chain model for both static and dynamic graph structures via simulations, showing the weaknesses and strengths of the mean-field approximation. We provide various insightful network simulations with links to videos, which lead to a number of corollaries. We also have explored quarantine control.

As was illustrated in Section IV-A, the n intertwined Markov chain model is a good approximation of the 2^n state model when β and δ are very different from each other. One could argue that the important cases are when β and δ are close to each other. Therefore, the question becomes: which of the two models better captures the true behavior of these systems? To answer this question requires real time series virus spread data, and it is possible that different models will perform better for different datasets.

In future work, we plan to address the questions posed above and further explore the development of optimal control methods. Exploring the existence and stability properties of the NDFE trajectory for the generic time-varying model is a problem that requires more investigation.

Acknowledgment

The authors would like to thank G. Dullerud, D. Liberzon, L. Feng, J. Liu, and S. Satpathi for several insightful discussions related to this work.

References

[1] D. Bernoulli, "Essai d'une nouvelle analyse de la mortalité causée par la petite vérole et des avantages de l'inoculation pour la prévenir," *Histoire de lAcad. Roy. Sci.(Paris) avec Mém. des Math. et Phys. Mém*, pp. 1–45, 1760.

[2] W. O. Kermack and A. G. McKendrick, "Contributions to the mathematical theory of epidemics. II. The problem of endemicity," *Proc. Roy. Soc. London Ser. A*, vol. 138, no. 834, pp. 55–83, 1932.

[3] A. Fall, A. Iggidr, G. Sallet, J.-J. Tewa, "Epidemiological models and Lyapunov functions," *Math. Model. Natural Phenom.*, vol. 2, no. 1, pp. 62–68, 2007.

[4] P. Van Mieghem, J. Omic, and R. Kooij, "Virus spread in networks," *IEEE/ACM Trans. Netw.*, vol. 17, no. 1, pp. 1–14, Feb. 2009.

[5] P. E. Paré, C. L. Beck, and A. Nedić, "Stability analysis and control of virus spread over time–varying networks," in *Proc. 54th IEEE Conf. Decision Control*, 2015, pp. 3554–3559.

[6] H. J. Ahn and B. Hassibi, "Global dynamics of epidemic spread over complex networks," in *Proc. 52nd IEEE Conf. Decision Control*, 2013, pp. 4579–4585.

[7] Y. Wang, D. Chakrabarti, C. Wang, and C. Faloutsos, "Epidemic spreading in real networks: An eigenvalue viewpoint," in *Proc. 22nd Int. Symp. Reliable Distrib. Syst.*, 2003, pp. 25–34.

[8] C. Peng, X. Jin, and M. Shi, "Epidemic threshold and immunization on generalized networks," *Phys. A: Stat. Mech. Appl.*, vol. 389, no. 3, pp. 549–560, 2010.

[9] S. Boyd, S.-J. Kim, L. Vandenberghe, and A. Hassibi, "A tutorial on geometric programming," *Optim. Eng.*, vol. 8, no. 1, pp. 67–127, 2007.

[10] V. M. Preciado, M. Zargham, C. Enyioha, A. Jadbabaie, and G. J. Pappas, "Optimal vaccine allocation to control epidemic outbreaks in arbitrary networks," in *Proc. 52nd IEEE Conf. Decision Control.*, 2013, pp. 7486–7491.

[11] V. M. Preciado, M. Zargham, C. Enyioha, A. Jadbabaie, and G. J. Pappas, "Optimal resource allocation for network protection against spreading processes," *IEEE Trans. Control Netw. Syst.*, vol. 1, no. 1, pp. 99–108, Mar. 2014.

[12] F. Pasqualetti, S. Zampieri, and F. Bullo, "Controllability metrics, limitations and algorithms for complex networks," *IEEE Trans. Control Netw. Syst.*, vol. 1, no. 1, pp. 40–52, Mar. 2014.

[13] A. Khanafer, T. Basar, and B. Gharesifard, "Stability properties of infected networks with low curing rates," in *Proc. Amer. Control Conf.*, 2014, pp. 3579–3584.

[14] A. Khanafer, T. Başar, and B. Gharesifard, "Stability of epidemic models over directed graphs: A positive systems approach," *Automatica*, vol. 74, pp. 126–134, 2016.

[15] C. Nowzari, V. M. Preciado, and G. J. Pappas, "Analysis and control of epidemics: A survey of spreading processes on complex networks," *IEEE Control Syst. Mag.*, vol. 36, no. 1, pp. 26–46, Feb. 2016.

[16] B. A. Prakash, H. Tong, N. Valler, M. Faloutsos, and C. Faloutsos, "Virus propagation on time-varying networks: Theory and immunization algorithms," in *Machine Learning and Knowledge Discovery in Databases*. New York, NY, USA: Springer, 2010, pp. 99–114.

[17] V. S. Bokharaie, O. Mason, and F. R. Wirth, "Spread of epidemics in time-dependent networks," in *Proc. 19th Int. Symp. Math. Theory Netw. Syst.*, vol. 5, no. 9, 2010, pp. 1717–1719.

[18] M. A. Rami, V. S. Bokharaie, O. Mason, and F. R. Wirth, "Stability criteria for SIS epidemiological models under switching policies," *Discrete Continuous Dynam. Syst. Ser.*, vol. 19, no. 9, pp. 2865–2887, 2014.

[19] M. R. Sanatkar, W. N. White, B. Natarajan, C. M. Scoglio, and K. A. Garrett, "Epidemic threshold of an SIS model in dynamic switching networks," *IEEE Trans. Syst., Man, Cybern., Syst.*, vol. 46, no. 3, pp. 345–355, Mar. 2016.

[20] Q. Liu, "The threshold of a stochastic susceptible-infective epidemic model under regime switching," *Nonlinear Anal.: Hybrid Syst.*, vol. 21, pp. 49–58, 2016.

[21] M. Ogura and V. M. Preciado, "Stability of spreading processes over time-varying large-scale networks," *IEEE Trans. Netw. Sci. Eng.*, vol. 3, no. 1, pp. 44–57, Jan.–Mar. 2016.

[22] S. Liu, N. Perra, M. Karsai, and A. Vespignani, "Controlling contagion processes in activity driven networks," *Phys. Rev. Lett.*, vol. 112, no. 11, 2014, Art. no. 118702.

[23] P. Holme, "Modern temporal network theory: A colloquium," *Eur. Phys. J. B*, vol. 88, no. 9, pp. 1–30, 2015.

[24] R. Pastor-Satorras, C. Castellano, P. Van Mieghem, and A. Vespignani, "Epidemic processes in complex networks," *Rev. Modern Phys.*, vol. 87, no. 3, p. 925, 2015.

[25] E. Valdano, L. Ferreri, C. Poletto, and V. Colizza, "Analytical computation of the epidemic threshold on temporal networks," *Phys. Rev. X*, vol. 5, no. 2, 2015, Art. no. 021005.

[26] C. Desoer, "Slowly varying system $\dot{x} = A(t)x$," *IEEE Trans. Autom. Control*, vol. AC-14, no. 6, pp. 780–781, Dec. 1969.

[27] F. Amato, G. Celentano, and F. Garofalo, "New sufficient conditions for the stability of slowly varying linear systems," *IEEE Trans. Autom. Control*, vol. 38, no. 9, pp. 1409–1411, Sep. 1993.

[28] X. Gao, D. Liberzon, J. Liu, and T. Başar, "Connections between stability conditions for slowly time-varying and switched linear systems," in *Proc. 54th IEEE Conf. Decision Control*, 2015, pp. 2329–2334.

[29] A. Ilchmann, D. H. Owens, and D. Prätzel-Wolters, "Sufficient conditions for stability of linear time-varying systems," *Syst. Control Lett.*, vol. 9, no. 2, pp. 157–163, 1987.

[30] P. A. Ioannou and J. Sun, *Robust Adaptive Control*. New York, NY, USA: Dover, 2012.

[31] V. Solo, "On the stability of slowly time-varying linear systems," *Math. Control Signals Syst.*, vol. 7, no. 4, pp. 331–350, 1994.
[32] S. Chatterjee and R. Durrett, "Contact processes on random graphs with power law degree distributions have critical value 0," *Ann. Probab.*, vol. 37, no. 6, pp. 2332–2356, 2009.
[33] R. A. Horn and C. R. Johnson, *Matrix Analysis*. Cambridge, U.K.: Cambridge Univ. Press, 2012.
[34] H. K. Khalil, *Nonlinear Systems*, vol. 3. Englewood Cliffs, NJ, USA: Prentice-Hall, 1996.
[35] T. H. Gronwall, "Note on the derivatives with respect to a parameter of the solutions of a system of differential equations," *Ann. Math.*, vol. 20, no. 4, pp. 292–296, 1919.
[36] R. Khasminskii, *Stochastic Stability of Differential Equations*, vol. 66. New York, NY, USA: Springer, 2011.
[37] J. Shi and J. Malik, "Normalized cuts and image segmentation," *IEEE Trans. Pattern Anal. Mach. Intell.*, vol. 22, no. 8, pp. 888–905, Aug. 2000.
[38] Y. Wan, S. Roy, and A. Saberi, "Network design problems for controlling virus spread," in *Proc. 46th IEEE Conf. Decision Control*, 2007, pp. 3925–3932.
[39] E. A. Enns, J. J. Mounzer, and M. L. Brandeau, "Optimal link removal for epidemic mitigation: A two-way partitioning approach," *Math. Biosci.*, vol. 235, no. 2, pp. 138–147, 2012.
[40] J. Hanna and A. Fantz, "Maine nurse won't submit to Ebola quarantine, lawyer says," March 19, 2015. [Online]. Available: http://www.cnn.com/2014/10/29/health/us-ebola/

Philip E. Paré received the B.S. degree in mathematics (Hon.) and the M.S. degree in computer science from Brigham Young University, Provo, UT, USA, in 2012 and 2014, respectively. He is currently working toward the Ph.D. degree in electrical and computer engineering at the University of Illinois at Urbana–Champaign, Urbana, IL, USA. His research interests include the modeling and control of dynamic networked systems, model reduction techniques, and time-varying systems.

Mr. Paré is a 2017–2018 College of Engineering Mavis Future Faculty Fellow.

Carolyn L. Beck received the B.S. degree from California Polytechnic State University, Pomona, CA, USA, the M.S. degree from Carnegie Mellon University, Pittsburgh, PA, USA, and the Ph.D. degree from California Institute of Technology, Pasadena, CA, USA, all in electrical engineering, in 1984, 1986 and 1997 respectively.

She is an Associate Professor with the Industrial and Enterprise Systems Engineering (IESE) Department, University of Illinois at Urbana–Champaign, Urbana, IL, USA. Prior to completing her Ph.D., she worked at Hewlett-Packard in Silicon Valley, CA, USA, for four years, designing digital hardware and software for measurement instruments. She has held visiting faculty positions at the Royal Institute of Technology, Stockholm, Sweden; Stanford University, Palo Alto, CA; and Lund University, Lund, Sweden. She has received national research awards and local teaching awards. Her research interests range from network inference problems to control of anesthetic pharmacodynamics. Her main research interests include model reduction and approximation for the purpose of feedback control design, mathematical systems theory, and clustering and aggregation methods.

Angelia Nedić received the Ph.D. degree in computational mathematics and mathematical physics from Moscow State University, Moscow, Russia, in 1994, and the Ph.D. degree in electrical and computer science engineering from Massachusetts Institute of Technology, Cambridge, MA, USA, in 2002.

She has worked as a Senior Engineer with the Advanced Information Technology Division, BAE Systems North America, Burlington, MA, USA. She is currently a faculty member of the School of Electrical, Computer and Energy Engineering, Arizona State University, Tempe, AZ, USA. Prior to joining Arizona State University, she was a Willard Scholar faculty member at the University of Illinois at Urbana–Champaign. Her general research interests include large-scale complex systems dynamics and optimization.

Dr. Nedić received the NSF CAREER Award 2007 in Operations Research for her work in distributed multiagent optimization. She is a recipient (jointly with her co-authors) of the Best Paper Award at the Winter Simulation Conference 2013 and the Best Paper Award at the International Symposium on Modeling and Optimization in Mobile, Ad Hoc and Wireless Networks 2015.